6-1992

Line Profile Asymmetries in Chromospherically Active Stars

Robert C. Dempsey
University of Colorado

Bernard W. Bopp
University of Toledo

Klaus G. Strassmeier
Universität der Vienna

Arno F. Granados
University of Colorado

Gregory W. Henry
Tennessee State University

See next page for additional authors

Recommended Citation

Dempsey, R.C.; Bopp, B.W.; Strassmeier, K.G.; Granados, A.F.; Henry, G.W.; Hall, D.S. "Line Profile Asymmetries in Chromospherically Active Stars" Astrophysical Journal v.392, p.187 (1992)

THE ASTROPHYSICAL JOURNAL, 392:187–200, 1992 June 10

LINE PROFILE ASYMMETRIES IN CHROMOSPHERICALLY ACTIVE STARS

ROBERT C. DEMPSEY[1]
Joint Institute for Laboratory Astrophysics, University of Colorado, Campus Box 440, Boulder, CO 80309
BERNARD W. BOPP[1]
Ritter Observatory and Department of Physics and Astronomy, University of Toledo, 2801 W. Bancroft, Toledo, OH 43606
KLAUS G. STRASSMEIER[1]
Institut für Astronomie, Turkenschanzstrasse 17, A-1180, Universität der Vienna, Austria
ARNO F. GRANADOS
Center for Astrophysics and Space Astronomy, University of Colorado, Boulder, CO 80309
GREGORY W. HENRY
Center for Excellence in Information Systems, Tennessee State University, 330 10th Avenue North, Nashville, TN 32703
AND
DOUGLAS S. HALL
Dyer Observatory, Vanderbilt University, Nashville, TN 37235
Received 1991 July 29; accepted 1991 December 10

ABSTRACT

A powerful, new probe of chromospheric activity—cross-correlation—has been developed and applied to a variety of stars. In this particular application, an entire CCD spectrum of an active star is correlated with the spectrum of a narrow-line, inactive star of similar spectral type and luminosity class. Using a number of strong lines in this manner enables the detection of absorption profile asymmetries at moderate resolution ($\lambda/\Delta\lambda \sim 40{,}000$) and S/N 150:1. This technique has been applied to 14 systems mostly RS CVn's, with $10 \leq v \sin i \leq 50$ km s^{-1} and $P \geq 7^{d}$. Distortions were detected for the first time in five systems: σ Gem, IM Peg, GX Lib, UV Crb, and ζ And. Detailed modeling, incorporating both spectral line profiles and broad-band photometry, is applied to σ Gem. Profile asymmetries for this star are fitted by two high-latitude spots covering 5% of the stellar surface. The derived spot temperature of 3400 K is lower than found in previous studies. In addition, two well-known systems have been studied: HD 199178 and V711 Tau. Polar spots are found on both.

Subject headings: line: profiles — stars: chromospheres

1. INTRODUCTION

For nearly two decades spot models have successfully reproduced the periodic brightness variations of RS CVn, BY Dra, W UMa, Algol, and even T Tauri stars (Eaton 1991). Spot longitudes, temperatures, and sizes can be obtained with reasonable accuracy from modeling multicolor light curves. However, such models suffer from nonuniqueness, and reliable latitude information is absent (Neff 1990; Strassmeier 1990). A major advantage to this technique is that photometry is relatively easy to obtain, especially with the advent of the Automatic Photoelectric Telescope (APT) Service (Genet et al. 1987).

Doppler imaging, wherein an absorption line profile is inverted to produce a temperature or brightness map of the photosphere, can yield reliable spot latitudes as well as detailed shape information (Deutsch 1970; Vogt & Penrod 1983). For a recent review of this technique applied to cool stars see Collier-Cameron (1991). An additional method for surface mapping results from the study of line curvature. Recently, Toner & Gray (1988) used high S/N and high-resolution spectra to study absorption line bisectors of ξ Boo A which exhibited periodic variations correlated with its 6.4 day rotation period, the latter inferred from Ca II emission flux variations. Their results were interpreted as the result of a "starpatch," characterized by enhanced macroturbulence, covering 10% of the visible disk.

Considering the potential of both methods it is perhaps surprising that these approaches have not been more widely applied. Since the spatial detail that can be extracted depends on the spectral resolution and the width of the line profile, Doppler imaging (DI) has been applied to only rapidly rotating stars ($v \sin i > 36$ km s^{-1}) with $\lambda/\Delta\lambda \sim 60{,}000$. Such a selection *excludes the vast majority of active stars.* Furthermore, the line distortions are at most only a few percent of the continuum, requiring S/N of typically 400:1 for modeling (Vogt, Penrod, & Hatzes 1987); a level not easily obtained at such high resolution. Due to these limitations, DI's great promise perhaps has faded, and only a handful of Doppler maps have been published: HD 199178 and V711 Tau (Vogt 1988), HD 26337 (Strassmeier 1990), HD 32918 (Piskunov, Tuominen, & Vilhu 1990), UX Ari (Vogt & Hatzes 1991), and HD 36705 (Kürster & Schmitt 1991). Bisector analysis, on the other hand, requires extremely sharp lines thus limiting one to, ideally, rotation speeds of less than a few km s^{-1}. Such a requirement restricts observations necessarily to *less active* stars while the need for resolving power $\sim$90,000 and S/N > 150:1 further limits the study to bright stars. Finally, blends present a serious problem for both techniques since clean unblended lines are required which are very difficult to

[1] Visiting Astronomer, Kitt Peak National Observatories, National Optical Astronomy Observatories, operated by the Association of Universities for Research in Astronomy, Inc., under contract with the National Science Foundation.

TABLE 1

TEMPLATE STARS

Name	Spectral Type	$v \sin i$
β Gem	K0 III	2.5
ϵ Cyg	K0 III	3.0
α Ari	K2 III	3.1
β Oph	K2 III	1.6
α Boo	K2 III	2.4
μ Her	G5 IV	1.1
ϵ Vir	G8 III	<8[a]

NOTE.—Values for $v \sin i$ are from Gray 1989, except that marked [a] which is from Bernacca & Perinotto 1973.

find in late-type spectra. However, problems produced by line blends can, in principle, be surmounted with more detailed model atmosphere calculations.

If a complete and consistent picture of stellar activity is to emerge, a large number of stars will have to be studied. To this end we have developed a new technique, correlative analysis (CA), to study profile asymmetries in the range of $15 < v \sin i < 40$ km s^{-1}. In this process, a narrow-line, template star is cross correlated with an active chromosphere star with the same spectral characteristics. The resulting cross correlation function (CCF) can then be inverted to study spot-induced profile asymmetries. The statistical advantage of utilizing the redundant information from many absorption lines. typically 20–30 strong ones, affords the observer the ability to detect asymmetries with lower S/N than is possible if only one of two profiles are fitted, as has been done to date in DI.

In this paper we report the application of CA to a number of stars using 0.11–0.38 Å resolution and 150:1 S/N. To illustrate the full potential of CA, a detailed spot model is presented for σ Gem.

2. OBSERVATIONS

2.1. *Spectroscopy*

Spectroscopic observations were obtained at three observatories over a 2 yr interval. The bulk of the observations were made with the Ritter Observatory 1 m telescope employing a fiber-coupled echelle and GEC CCD (Bopp, Dempsey, & Maniak 1988; Bopp et al. 1989). The fainter stars ($V > 6$ mag) were primarily observed with the coudé feed spectrograph at Kitt Peak National Observatory (KPNO) during two observing runs in 1990 March and May. An 800 × 800 (15 μm pixels) TI CCD was used with grating A and camera five. Additional data were obtained through the McMath stellar synoptic program for two stars: HD 199178 (V1794 Cyg) and V711 Tau (HR 1099). This system utilizes a TI 800 × 800 thinned CCD (15 μm square pixels) in conjunction with a Milton-Roy grating.

In all, a total of about 350 spectra were obtained for 16 program and 10 template stars. Tables 1 and 2 list the properties of the template and program stars, respectively. A journal of observations is given in Table 3. Program stars were chosen primarily from the catalog of chromospherically active binary stars (=CABS; Strassmeier et al. 1988a). These stars were chosen for their strong Ca II H and K emission fluxes or large photometric amplitudes or both.

Data for the photometric amplitude (ΔV), the photometric

TABLE 2

PROGRAM STARS

	Star	Spectral Type	$v \sin i$ (km/s^{-1})	P[a] (d)	ΔV (mag)	Temp
ζ And	HD 4502	K1 IIe	36	17.8[b]	0.0	α Ari α Boo
ι Tri	HD 13480	? + G5 III	30	14.73[b]	0.0	μ Her
V711 Tau	HD 22478	G5 IV + K1 IV	38	2.841	0.22	α Ari
V492 Per	HD 28591	K1 III	24	21.3	0.07	α Ari
BM Cam	HD 32357	K0 III	15	80.94	0.14	β Gem
σ Gem	HD 62044	K1 III	25	19.410	0.06	β Gem
DQ Leo	HD 102509	G5 IV–III	15	71.69	0.03	μ Her
BM CVn	HD 116204	K1 III	15	21.7	0.06	α Boo
ι Vir	HD 124850	F6 III	17[c]	7.0	0.05	ι Vir[d]
UV CrB	HD 136901	K2 III[e]	42	18.668	0.163	α Boo
GX Lib	HD 136905	K1 III	32	11.134	0.1	α Boo
ϵ UMi	HD 153751	G5 III	24	39.48[b]	0.0	μ Her
HD 199178	V1794 Cyg	G5 IV	74[f]	3.337	0.08	μ Her α Ari
o Dra	HD 175306	K0 III	16[f]	54.6:	0.034	ϵ Cyg
IM Peg	HD 216489	K1 III	24	24.349	0.16	α Ari α Boo
λ And	HD 222107	G8 IV–III	10	53.952	0.28	ϵ Vir

NOTE.—Temp is the star used for the cross correlation.
[a] Photometric periods.
[b] Orbital period, $P_{ph} \sim 0.5 P_{orb}$.
[c] Soderblom et al. 1989.
[d] No template available.
[e] Fekel et al. 1989.
[f] This paper.

TABLE 3

JOURNAL OF OBSERVATIONS

Star	Dates	n	Telescope
ζ And	1990 Jan 7–Feb 5	2	RO
	1990 May 15–May 17	3	CF
BM Cam	1988 Dec 7–1989 Jan 22	3	RO
	1990 Mar 3–Mar 7	2	CF
o Dra	1989 Jun 7–Sep 27	5	RO
σ Gem	1989 Jan 10–Apr 22	14	RO
	1989 Dec 15–1990 Mar 2	8	RO
	1990 Mar 3–Mar 7	4	CF
	1990 May 15	1	CF
V492 Per	1990 Mar 3–Mar 7	3	CF
UV CrB	1990 Mar 3–Mar 7	2	CF
	1990 May 15–May 19	7	CF
GX Lib	1990 Mar 3–Mar 7	2	CF
	1990 May 15–May 19	7	CF
BM CVn	1990 Mar 3–Mar 7	2	CF
IM Peg	1989 Dec 1–1990 Jan 25	4	RO
	1990 May 15–May 19	2	CF
V711 Tau	1988 Oct 14–1989 Sep 21	14	MC
	1988 Dec 30–1989 Jan 23	0	RO
	1990 Mar 3–Mar 7	2	CF
ι Tri	1989 Jan 22	0	CF
	1989 Nov 30–1990 Jan 8	3	RO
ε UMi	1989 Apr 16–Jul 10	2	RO
DQ Leo	1989 Jan 23–Jun 7	4	RO
HD 199178	1989 Apr 28–Sep 22	15	MC
	1990 May 15–May 9	5	CF
λ And	1989 Jul 8–Sep 27	8	RO
	1990 Jan 8	1	RO
ι Vir	1989 Apr 20–Jul 10	6	RO

NOTE.—RO refers to Ritter Observatory, CF the coudé feed at KPNO, and MC designates the McMath synoptic observations. For RO observations, each observation refers to three echelle orders.

period (P_{ph}), v sin i, and spectral class used throughout the analysis are primarily from the CABS catalog. P_{ph} for HD 199178 was taken from Jetsu et al. (1990), while ΔV for this star was obtained from contemporaneous APT photometry. Relevant data for ι Vir comes from the Bright Star Catalog (Hoffleit 1982) and Noyes et al. (1984). For ζ And, ι Tri, and ε UMi, CABS lists ΔV as zero, since the photometric variability is supposedly dominated by ellipticity and reflection effects, but a small amount of modulation in the first two systems may be due to spots (Strassmeier et al. 1989). The rotation period for UV CrB is from Hall (1990). Values of ΔV for IM Peg and Gem are also from concurrent APT data (Dempsey 1991).

Appropriate template stars were observed each night to check the quality of the data, to gauge activity levels and to be used in the cross correlation. These stars were chosen for their low levels of activity as indicated by weak or absent Ca II H and K emission and because they had spectral types similar to those of the program stars. It is important that the template stars possess narrow-line profiles as broad lines will smooth or wash out detail in the resultant CCF. Therefore all the template stars were required to be slow rotators (v sin $i < 3$ km s^{-1}). No appropriate template was available for ι Vir so the first spectrum of ι Vir was taken as the template. This is sufficient to detect relative changes but due to the broader lines of the "template" the sensitivity is reduced.

The choice of wavelength regions was dictated by the need for many strong absorption lines as free from telluric contamination as possible. While blends present no difficulty in CA, telluric lines introduce uncorrelated signals that may wash out subtle asymmetries. Therefore, the wavelength regions were chosen to be as free from telluric contamination as possible. For the Ritter observations, the spectra covered three regions: $\lambda\lambda$6395–6425, 6210–6245, and 6050–6080. Resolution, defined as the full width at half-maximum (FWHM) of several narrow comparison lines, was 0.11 Å for the Ritter observations, except for IM Peg where 0.38 Å was used. Both the McMath and KPNO data cover 80 Å with a resolution of 0.15 Å and 0.27 respectively. S/N was $\geq$150:1 in all cases.

All data were reduced in standard fashion (i.e., bias subtraction to remove DC level, flat-fielded to remove pixel-to-pixel variations, etc.) with IRAF.[2] Th-Ar spectra were obtained nightly for wavelength calibration.

2.2. *Photometry*

Supplementary photometry was obtained for three stars which exhibited very interesting line profile variations: σ Gem, ζ And, and HD 199178. Johnson V and B data were obtained with the Vanderbilt-Tennessee State 0.4 m APT (Gent et al. 1987). The ephemeris 2,444,686.5 + 19.410E (Strassmeier et al. 1988b) was adopted for σ Gem, and the data were obtained during the interval HJD 2,447,893–2,448,028. Phases for HD 199178 were computed from Jetsu et al.'s (1990) ephemeris of 2,444,395.78 + 3.337484E. Photometric data for HD 199178 were obtained approximately nightly from HJD 2,447,647 to 2,447,882. Data for ζ And cover the intervals HJD 2,447,115–2,447,203 and 2,448,062–2,448, 258.

3. CORRELATIVE ANALYSIS

Vogt & Penrod (1983) indicated how a region in the stellar photosphere with a different temperature, either higher or lower, could distort the line profile. If we ignore changes in equivalent width inside of these regions, a reasonable assumption in most cases (Vogt et al. 1987 and Strassmier 1990, but also see Piskunov et al. 1990 and Strassmeier et al. 1991), then the strength of the bumps is dominated by the longitudinal extent of the spots, i.e., a purely geometric effect that affects all lines. The advantage of cross correlation is that it utilizes the information contained in *all* of the lines in calculating the CCF, which is essentially a mean profile. Of course, not all lines are affected in exactly the same manner, owing to their different strengths and temperature sensitivities, but enough strong lines of similar character will dominate the CCF to yield the desired result.

Before the cross-correlation function can be calculated it is necessary to prepare the data in several ways. Any residual curvature in the continuum is removed by dividing the data with a low-order polynomial that is fitted to the continuum. To avoid the need for windowing (see Bendat & Piersol 1986), the ends of the wavelength region are chosen to correspond to the local continuum so there is no discontinuity at the edges. All Doppler shifts are removed to ensure that each CCF corresponds to exactly the same wavelength coverage for both the template and program star at all epochs. The CCFs were calculated according to Bendat & Piersol (1986) with further details given in Dempsey (1991).

[2] IRAF is distributed by National Optical Astronomy Observatories, which is operated by the Association of Universities for Research in Astronomy, Inc., under contract with the National Science Foundation.

To illustrate the process, Figure 1 displays typical spectra of V711 Tau and the template star, α Ari, used in the cross correlation. Asymmetries that are clearly present in the profiles of V711 Tau are reflected in the CCF. Note that the x-axis of the CCFs is in lag units or Å. In this portion of the spectrum, chosen to avoid phases where the profiles from both binary components overlap, only two lines, Fe I λ 6431 and Ca I 6439 Å, from both components are visible. Both lines have been used previously in Doppler imaging studies (e.g., Strassmeier 1990).

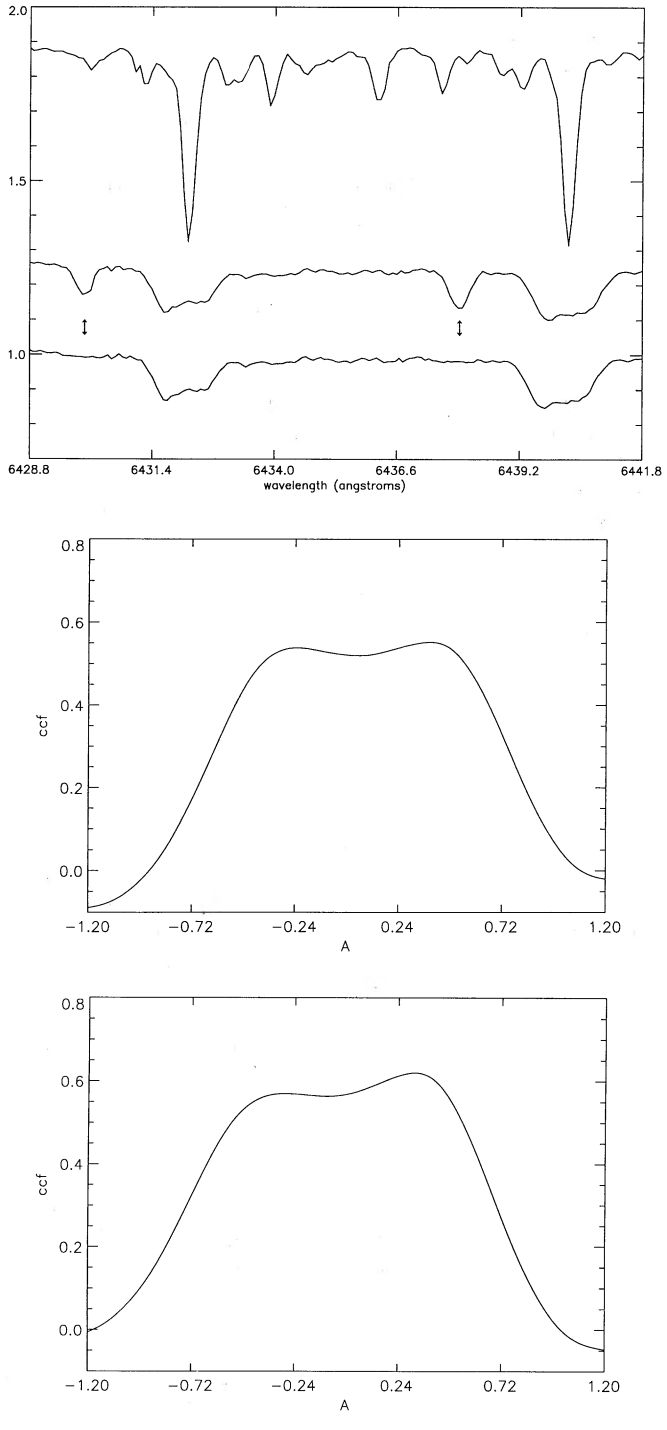

FIG. 1.—*Top*: Normal stellar spectra for the template α Ari and V711 Tau in the top and middle spectra, respectively. Removal of the secondary lines is seen in the bottom spectrum. *Middle*: CCF that results from the normal spectra. *Bottom*: CCF resulting from correlating with the "cleaned" spectrum. Spectra have been normalized to unit continuum intensity but shifted arbitrarily in the vertical direction. *Note how a "bump" on the redward side of the line profile translates into a depression on the left of the CCF.*

In ι Tri and V711 Tau, lines from secondary components are visible. This produces problems because the profiles of the template will not correlate well with the "profile" of the program star resulting in degradation of the CCF. To minimize this effect, a window containing only two clearly separated sets of lines (two from each star) was chosen, and the secondary's features were deleted to approximate a single-limited spectrum. This does not correct for the effect of the secondary's continuum on the profile of the primary. Overlapping profiles for V711 Tau were ignored. Future development will allow the proper evaluation of double-lined spectra by utilizing an artificial double-lined spectroscopic binary standard.

4. CROSS-CORRELATION RESULTS

4.1. *The Fiduciary Systems: V711 Tauri and HD 199178*

Before the results can be interpreted it is important to ascertain the effectiveness of our cross-correlation technique. To do this, two well-studied systems, V711 Tau and HD 199178, were included in the program. A summary of relevant properties is found in Table 2.

CCF results for all of the V711 Tau data are shown in Figure 2. Several things are worth noting. One element common to all the CCFs is a depression at the center of the CCF. While it is not possible to draw firm conclusions without detailed modeling, such a profile shape is consistent with the interpretation that a large spot, covering the pole and therefore always in view, is present as suggested by Vogt & Penrod (1983), Jankov & Foing (1987), and Vogt (1988). Such behavior has also been observed on HD 199178 (Vogt 1988) and HD 26337 (Strassmeier 1990).

Two observations at phase 0.758, but separated in time by two and a half weeks (~6 rotations), turn out to be identical. While easily seen in the CCFs it is more difficult to see in the actual spectra, showing how effective this method is in studying asymmetries. This suggests that the spot configuration can be stable for more than six rotations. The other asymmetries present in the CCF result from lower latitude spots. Detailed Doppler imaging of the same data confirm these conclusions (Donati, et al. 1992).

The second benchmark system, HD 199178, is different from V711 Tau in that it is an apparently single G5 IV star of the FK Com class (Bopp 1982). Although DI studies require a large v sin i to obtain high spatial resolution, as v sin i increases, the asymmetry becomes an ever increasingly smaller percentage of the line profile. Thus, very high S/N, typically greater than 300:1, is required to detect the asymmetries. Comparing broadened high-resolution spectra of μ Her (G5 IV) and δ CrB (G5 III–IV) to that of HD 199178 in this study yields v sin $i = 74 \pm 2$ km s^{-1}. Figure 3 displays a typical spectrum of HD 199178. Here the S/N is about 150:1, considerably less than required for DI. The resulting CCFs are displayed in Figure 4. *Asymmetries which are undetectable with the unaided eye in an individual absorption profile are clearly evident in the CCF.* Therefore, through correlative analysis *asymmetries can be reliably analyzed at much lower S/N than previously possible using only one or two profiles.*

Again, there is the near continuous presence of a central

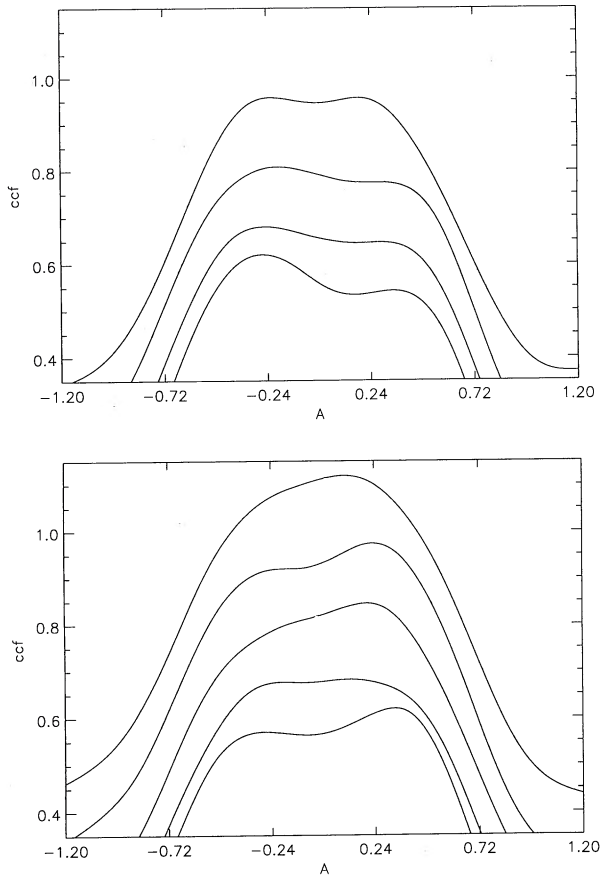

FIG. 2.—Cross-correlation results for V711 Tau. Each correlation function has been arbitrarily shifted in the vertical direction for ease of visualization. From bottom to top rotational phases, ϕ, are 0.182, 0.364, 0.396, 0.436, 0.459, 0.732, 0.758, 0.758, and 0.822. The data cover the interval HJD 2,447,449–2,447,791.

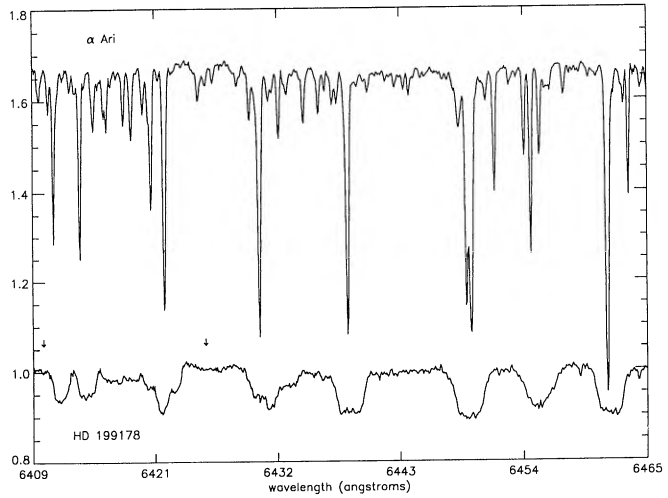

FIG. 3.—Spectrum of HD 199178 around 6440 Å. With $v \sin i = 74 \pm 2$ km s^{-1} the lines are very shallow and the profile asymmetries are hard to detect from visual inspection. Arrows denote the wavelength region used. α Ari, used as the McMath template, is shown at the top. While this spectrum is relatively free from telluric features, others frequently contained many such features redward of λ6440.

depression at all phases which is consistent with the presence of a large polar spot as supported from DI (Vogt 1988) or, at the very least, a high-latitude spot. However, unlike V711 Tau, *changes on short time scales* are visible. The rotation period of HD 199178 is 3^d.33 and our observations extend over many months. As can be seen in Figure 4, CCFs with similar phases, but obtained weeks apart, display very different shapes. For example the two CCFs at $\phi = 0.33$ are 9 days apart (<3

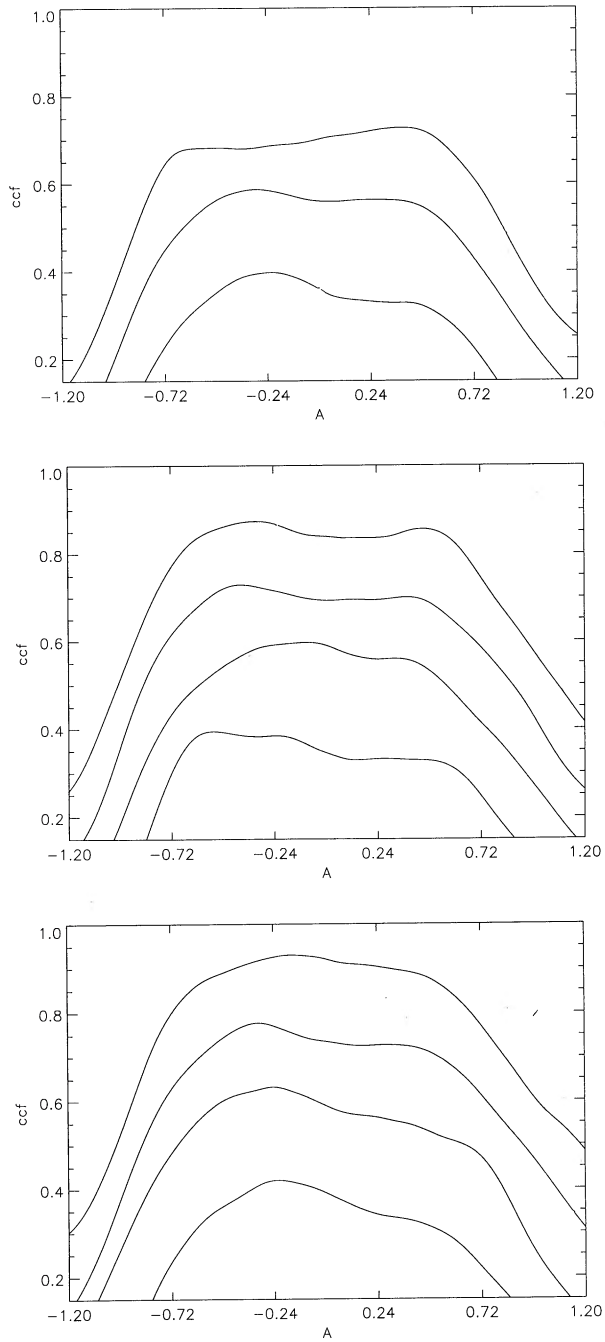

FIG. 4.—CCF results for *all* McMath HD 199178 data ordered in phase. Phases from bottom to top are 0.14, 0.45, 0.75, 0.24, 0.33, 0.62, 0.84, 0.29, 0.33, 0.71, and 0.86. α Ari (K2 III) was used as the template for all the McMath data. CCFs have been shifted in the vertical direction for clarity. Data cover the interval HJD 2,447, 672–2,447,792.

rotations) but are markedly different. After analyzing the photometry it was decided to break the data up to three epochs. Light curves for these intervals are displayed in Figure 5.

Of course these subsets are rather artificial since the spot distribution is probably evolving continuously. Comparing Figure 4 and Figure 5, one notes that the strong asymmetry on the blue side of the peak at $\phi = 0.14$ corresponds to photometric minimum while at maximum light there is a pronounced asymmetry on the red side. Within a rotation or two, the spot configuration has changed as seen in both the light curve and the CCFs. After this time the light curve continued to change, rapidly reaching an amplitude of 0.2 mag by HJD 2,447,000 compared to 0.06 mag 100 days before (Fig. 5).

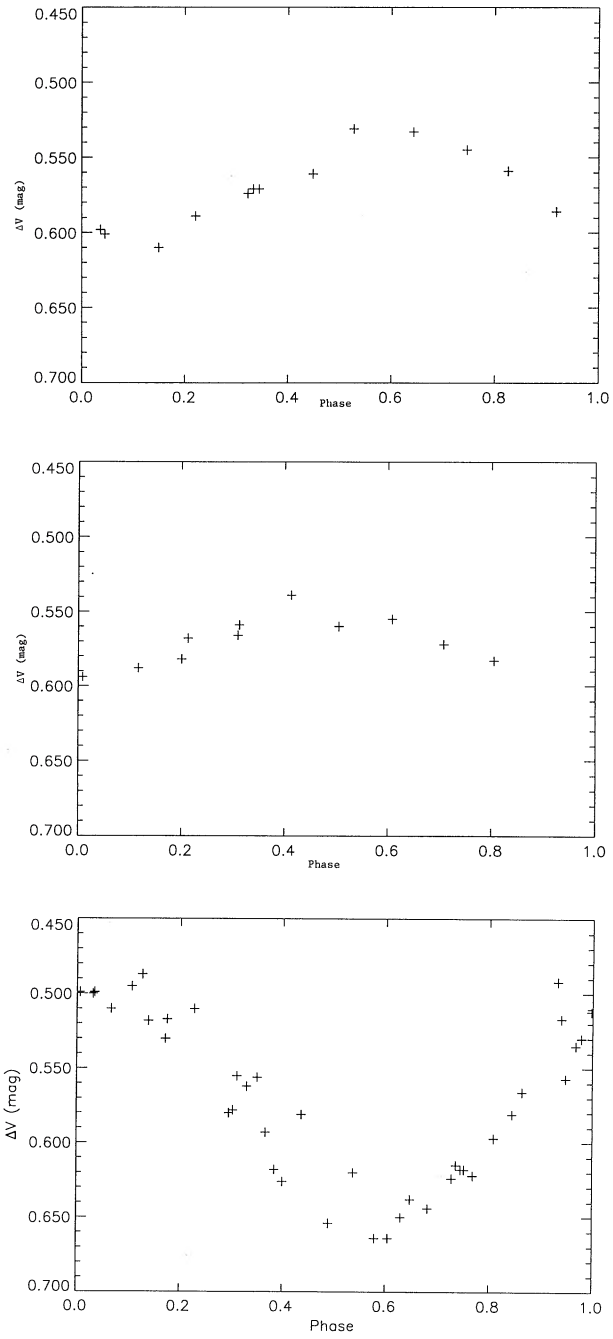

FIG. 5.—Light curves for HD 199178. *Top*: Data from the interval HJD 2,447,600–2,447,674 corresponding to the top panel of CCFs in Fig. 4. *Middle*: Data from the interval HJD 2,447,674–2,447,700 corresponding to the middle panel of CCFs in Fig. 4. *Bottom*: Data from the interval HJD 2,447,700–2,447,882 corresponding to the bottom panel of CCFs in Fig. 4.

The data in Figure 6, taken over a 5 day interval at KPNO, show good coverage over one complete rotation. These data were taken 10 months (91 rotations) later than the McMath data shown in Figure 4. Here the resolution is slightly lower so the amplitude of any asymmetry will necessarily be smaller. Note also that the template star was μ Her which more nearly matches HD 199178 in spectral type. Comparing Figure 6 with Figure 4, it is apparent that changes have again occurred in the spot configuration but the high-latitude spot is still present.

Figure 4 points out the effect of spectral-type mismatch. While HD 199178 is listed as mid-G or G8 III by Fekel (1991), only α Ari (K2 III) was available for comparison for the McMath data. This is still a sufficient template to detect the asymmetries. However, due to differences in absorption line depths between the template and program star there is a tendency for the CCF to slope to the right. The slope was not present in the KPNO cross correlations where μ Her (G5 IV) was the template star. It is important to remember that, while such mismatch *may introduce systematic effects, it cannot produce changes seen from night to night.*

4.2. *Bisectors*

While there is no doubt that the profile variations seen in V711 Tau and HD 199178 are real, care must be exercised to ensure that the more subtle asymmetries seen in stars like σ Gem are indeed real. To more easily characterize subtle changes it was decided to calculate the bisector of the CCF. Here the bisector is the locus of points lying midway between points of equal amplitude on each side of the CCF which divides the peak into halves of equal area. *It cannot be over*

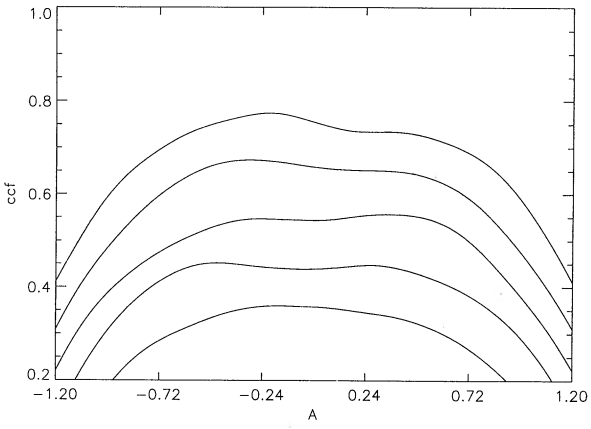

FIG. 6.—Cross-correlation functions for HD 199178 over the interval HJD 2,448,026–2,448,031. These data are from Kitt Peak and follow the McMath data by 10 months. Note that the structure is basically the same. The phases are from bottom to top 0.09, 0.22, 0.53, 0.82, 0.92. Scale is the same as in the previous figures for comparison. The fact that there is nearly always a depression near the center of the CCF is consistent with the presence of a polar spot. Other changes are apparently due to other smaller spot groups passing in and out of view. Recall that the resolution here is lower than for the McMath data. In this case, μ Her (G5 IV) is the template star which has a spectral type closer to that of HD 199178. Note the difference in the CCF from $\phi = 0.82$ to that of the CCFs in Fig. 4 with nearly the same phase. Concurrent photometry was unavailable for comparison.

emphasized that these bisectors quantify only the profile asymmetry of the CCF and should not be confused with bisectors used by Toner and Gray (1988) which measure velocity fields in the photosphere. As discussed in § 5, due to spectral type mismatch, it is more convenient to model the bisectors rather than the whole CCF.

Since spectral type mismatch may induce slight asymmetries in the CCF, and this should occur only in the worst cases like HD 199178 where a more appropriate template was unavailable, true profile asymmetries can be identified by their *temporal variations.* To quantify these effects, three quantities were measured. For each bisector the mean and standard deviation in the lag of 10 points located near half the peak value of the CCF were calculated. This standard deviation, σ_B, measures the linearity of the bisector. The lag difference between the mean of the top 10 points of the bisector and the above mean, Δ, is also measured. Therefore, the ratio of the maximum Δ to the maximum σ_B is an estimate of the largest degree of asymmetry. Polar spots are not detectable in this manner but can be inferred from the height of the CCF peak. Values of Δ, σ_B, and the ratio $\gamma \equiv \max(\Delta)/\max(\sigma_B)$ are listed in Table 4. There is a large gap from $\gamma = 50$–100 and systems like σ Gem, IM Peg, and GX Lib, which visibly show bisector variations, all have $\gamma > 100$. Therefore, $\gamma = 100$ is taken as the cutoff delineating positive systems, i.e., those which show profile variations, from those that show no variations. One exception is V492 Per whose large γ is the result of the very small σ_B, the lowest for all the systems, and it sould be recognized that Δ is smaller than the "positive" systems by more than a factor of 5.

Is it possible that the detection or nondetection of profile variations is the result of the template star used in the correlation? While the template stars may be active at some level it seems unlikely that any effects could be seen in the narrow lines of the standards ($v \sin i < 3$ km s^{-1}) where mechanisms other than rotation dominate line broadening. It is hard to imagine any temperature inhomogeneity large enough to disturb the profile but not show itself through other ways such as photometric modulation. In addition, the same templates were sometimes used for different stars with and without profile asymmetries. Contemporaneous Hα and Ca II λ8542 observations of the standard stars revealed a lack of emission or variation (Dempsey 1991). Finally, cross-correlating the template stars with other template stars did not reveal any variations.

TABLE 4

SUMMARY OF BISECTOR RESULTS

Star (1)	σ_B mÅ (2)	Δ mÅ (3)	γ (4)
Positive Detections			
σ Gem	0.18	29	161
IM Peg	0.28	37	132
GX Lib	0.13	41	315
ζ And	0.18	39	217
UV CrB	0.34	102	300
Negative Detections			
λ And	0.12	1	8
DQ Leo	0.19	2	19
o Dra	0.34	17	49
ι Vir	0.11	5	43
BM Cam	0.13	4	28
V492 Per	0.03	6	187
BM CVn	0.13	4	33
ϵ Umi	0.68	24	35

NOTE.—Cols. (2) and (3) list the *maximum* values of all observations for a given star.

Out of 16 objects, seven, including V711 Tau and HD 199178, displayed some sort of profile variations. For the other five we note that this is the *first* detection of asymmetries in stars with rotation periods longer than 10 days. A more detailed discussion of the rest of the systems with positive detections follows.

4.3. *Systems with Newly Detected Profile Distortions*

4.3.1. σ *Geminorum*

Classified as a long-period RS CVn by Hall (1976), σ Gem has been studied extensively spectroscopically and photometrically. Strassmeier et al. (1988b), Fried et al. (1983), and Olah et al. (1989) have modeled a large body of photometric data extending over a decade. These groups found that the σ Gem light curves can always be fitted with two spots that migrate in longitude. Spot area appears to vary regularly with a period of $\sim$2.7 yr (Strassmeier et al. 1988b). Eker (1986) examined spectral-line variations. Although his data resolution was too low to detect profile asymmetries, he did note changes in the equivalent widths of some lines. Temperature sensitive lines like Ca I 6572.8 were observed to deepen at the same time that the Hα core emission increased. He further found the Hα emission to be correlated with phase. Bopp et al. (1988) also observed changes in the residual intensity of the Hα line that were phase-dependent but for only one of the two observing seasons discussed. Variations in Hα equivalent width detected by several groups (Bopp & Talcott 1980; Smith & Bopp 1982 and Strassmeier, Weichinger, & Hanslmeier 1986) indicate that the star is quite variable. No profile distortions were detected by Eaton (1990) with spectra having resolving power $\lambda/\Delta\lambda \sim 4 \times 10^4$.

Typical spectra are plotted in Figure 7. The cross-correlation function of the 6420 Å region spectrum is plotted in Figure 8 with its resulting bisector. While the magnitude of the asymmetry in the CCF is considerably less than for V711 Tau and much harder to detect with the eye, the asymmetries are clearly reflected in the cross-correlation functions. Note that a depression on the blue side of the CCF will make the bisector curve redward. For comparison, a CCF and its bisector for V492 Per are shown in Figure 9. Its spectral type and $v \sin i$ are identical to that of σ Gem but no profile asymmetries were detected in the five observations of this star that extended over one-quarter of a rotation cycle. The resulting bisectors for σ Gem, arranged according to phase, are displayed in Figure 10. Observations from KPNO are included as well. Bisectors for the other wavelength regions of the Ritter echelle data are not shown since the behavior is similar.

As mentioned previously, Eker (1986) noted changes in equivalent width in some of the absorption lines of σ Gem. He found the stronger lines to be insensitive to temperature changes while weaker lines varied in equivalent width by as much as 8%. The spectra obtained for the cross correlations contain features that possess a wide range of strengths and sensitivity to temperature. Some of these lines are designated *W* and *S* (Moore, Minnaert, & Houtgast 1966) indicating weakening or strengthening in sunspots. Careful examination of spectra roughly corresponding to brightness maximum and

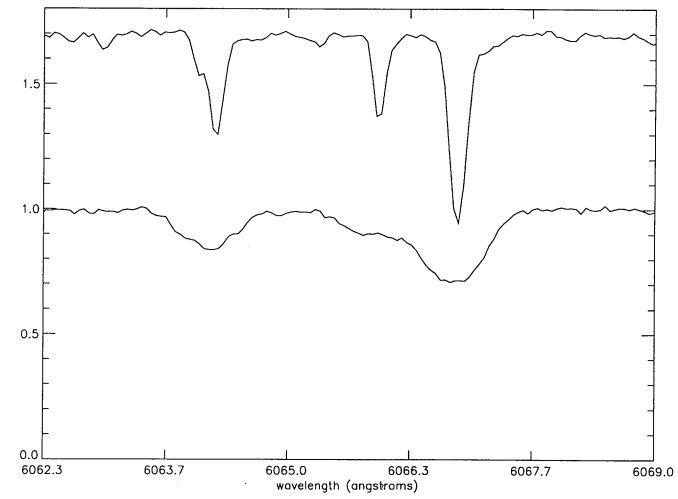

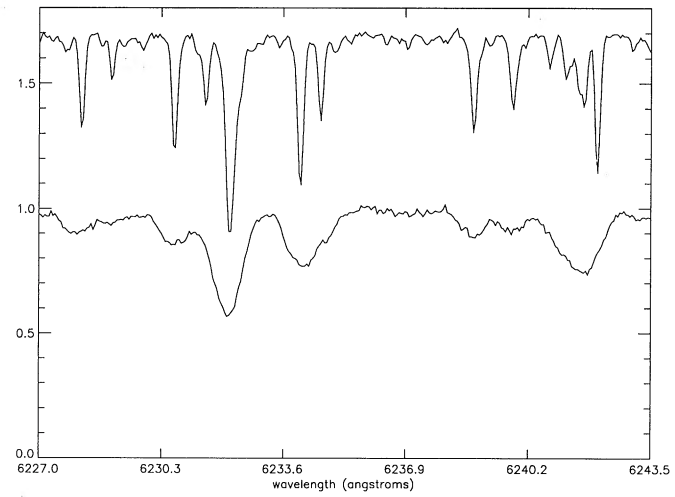

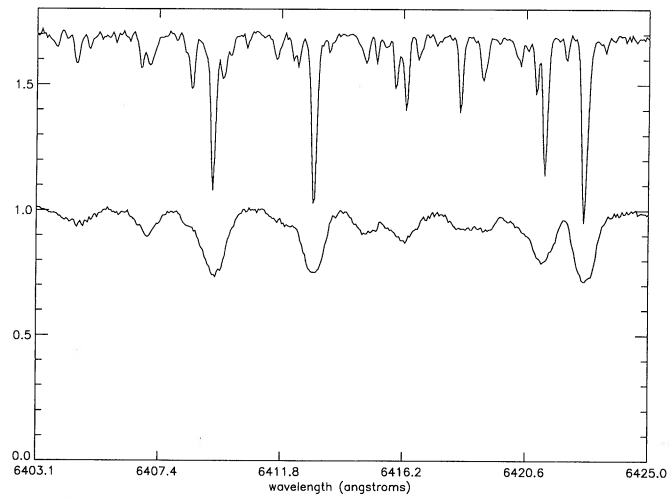

FIG. 7.—Spectra of σ Gem for three echelle orders from $\phi = 0.42$. The top spectrum in each frame is that of the standard star β Gem, used for cross-correlating σ Gem. β Gem has been shifted arbitrarily in the y-direction after normalization to unit continuum intensity.

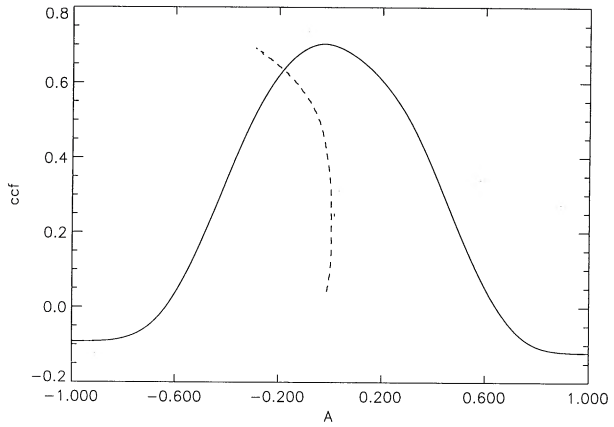

FIG. 8.—CCF of 6420 Å order for σ Gem and its bisector (*dashed line*). Note that the x-scale of the bisector has been multipled by 10 to make it easier to see the curvature.

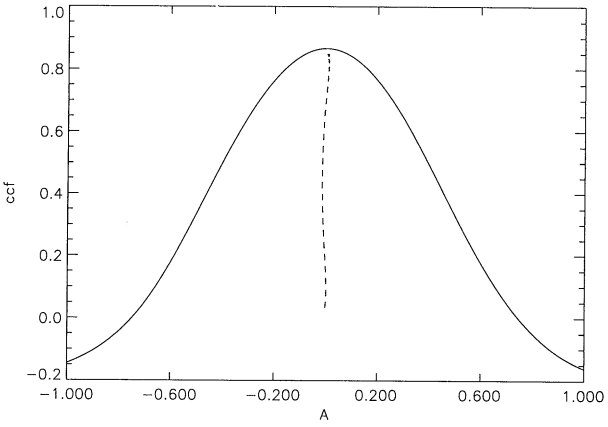

FIG. 9.—Cross correlation and bisector for V492 Per. Note that the x-scale of bisector has been multiplied by 10. There is no significant curvature.

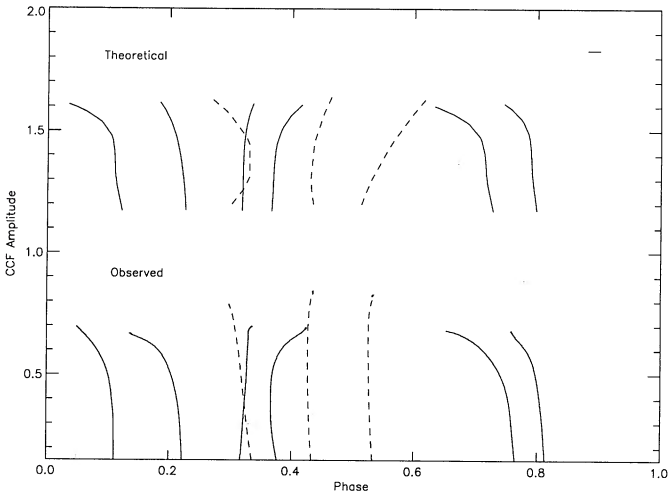

FIG. 10.—Bisectors for σ Gem ordered in phase. Dashed lines designate KPNO data and the increased height results from different resolution which affects the normalization of the CCF (see Bendat & Piersol 1986). Data along the bottom are the observed bisectors resulting from cross-correlating σ Gem with β Gem. The bisectors in the top row have been shifted vertically by unity and result from the theoretical model discussed in § 5 (Fig. 17). A horizontal bar in the upper right represents 0.1 Å in lag for scale. Data correspond to the interval HJD 2,447,910–2,447,956.

minimum reveal no changes similar to those observed by Eker. Photometry that is contemporaneous with Eker's observations (Strassmeier et al. 1988b) indicate an amplitude of ~0.12 mag, which is larger than that observed during the 1989–1990 season discussed here. Since Eker's spectra were of lower resolution, the lack of any variation seen here must be due to lower surface activity, or a less asymmetrical distribution of active complexes. While failing to detect such equivalent width changes may seem disappointing, it serves further to emphasize how *the CCF technique detects changes that would be missed by other more conventional methods.*

4.3.2. *IM Pegasi (HR 8703)*

Like σ Gem, IM Peg is a long-period RS CVn system, but with a higher level of chromospheric activity as indicated by stronger Ca II emission and weaker Hα absorption. According to Strassmeier et al. (1989), light curves of IM Peg are typically asymmetric with amplitudes around 0.2 magnitudes while Hall (1981) noted an amplitude range of 0.16–0.23 mag. Solutions of the light curves alone suggest the presence of two spots covering about 6% of the surface (Poe & Eaton 1985).

Observations of absorption line profile variability began in 1989 December and could be continued only through 1990 January. Unfortunately, the faintness of the object ($V = 5.57$) precluded use of the highest Ritter spectral resolution. Since profile changes were detectable in σ Gem, a considerably less active star, it was decided to observe IM Peg at lower resolution (~0.38 Å). Even at this reduced resolution, the cross-correlation technique was able to detect marked profile asymmetries (Fig. 11). Two additional observations were obtained at KPNO in 1990 May. Despite limited phase coverage, two important effects can be seen in the data. First, deviations from a straight bisector reach 7 mÅ, which is about twice the maximum excursion for σ Gem. Also the bisector at phase 0.74 exhibits significant deviation from a straight line farther down the bisector (i.e., farther from line core) than for any other star. This indicates the presence of a large spot on the approaching limb.

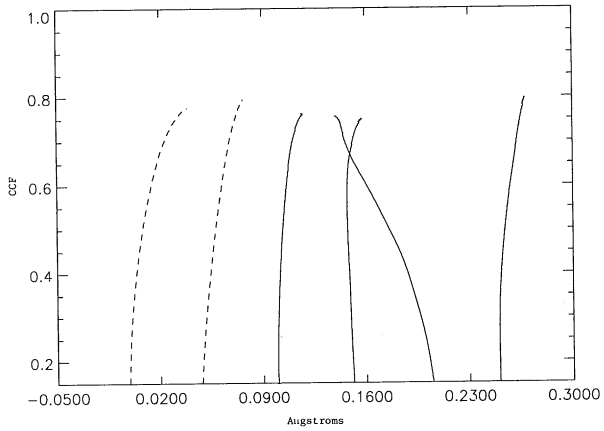

FIG. 11.—Bisectors from the 6420 Å region of IM Peg. Two bisectors from KPNO are also included as dashed lines. Phases, from left to right, are 0.13, 0.17, 0.60, 0.68, 0.74, and 0.90. Note the change of scale from Fig. 10 in that the bisectors are plotted vs. lag in units of Å. Bisectors have been shifted arbitrarily for clarity. α Boo is used for correlation of the KPNO data, while α Ari is the Ritter template for IM Peg. The data cover an interval of HJD 2,447,861–2,448,028.

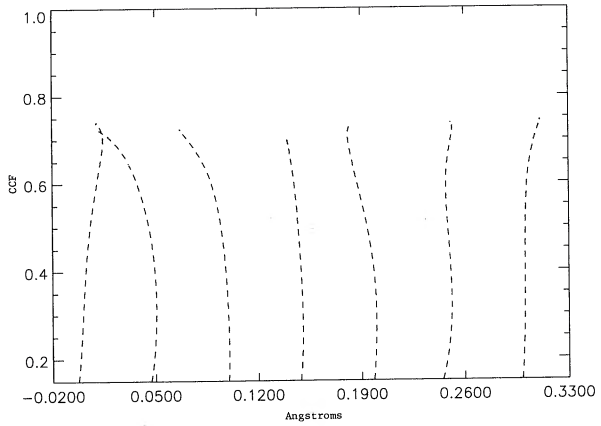

FIG. 12.—Bisectors of GX Lib. Phases have been computed with Fekel et al.'s 1989 orbital period and phase zero corresponds to the first observation. Phases, from left to right, are 0, 0.27, 0.44, 0.53, 0.63, 0.17, and 0.80. All data are from KPNO and cover the interval HJD 2,447,954–2,448,031. Axes and arrangement follow the convention of Fig. 11.

4.3.3. *GX Librae (HD 136905)*

Another star which exhibits profile variations is GX Lib. Discovered as photometrically variable by Burke et al. (1982), it has been further studied by Bopp et al. (1983), Fekel, Moffett, & Henry (1986), and Strassmeier et al. (1989). These studies concluded that the photometric variability was primarily a result of the ellipticity effect. However, Strassmeier et al. (1989) noted changes in the brightness of the photometric maxima, suggesting the presence of a spot component as well. Resulting bisectors are displayed in Figure 12. When arranged in phase, a sequence very similar to that for σ Gem (Fig. 10) is observed. Seven observations over five nights cover about one-half of a rotation cycle with observations obtained on the same night yielding identical bisectors. The two observations at phases 0.0 and 0.27 were obtained about six rotation cycles prior to the others. Although subtle, the bisector variations *confirm the presence of small spots* on GX Lib.

4.3.4. *ζ Andromedae*

A number of investigators, summarized in Strassmeier et al. (1989), have studied the photometric variability of ζ And, concluding that the changes are due to ellipsoidal variations and the reflection effect. From the analysis of the ellipticity effect, Hall (1990) determined a radius for the primary equal to 80%–100% of its Roche lobe radius, $R_{\rm Roche}$. He also showed that the unequal minima result from limb-darkening effects on the pointed end of the elongated star, not from reflection. However, Strassmeier et al. (1989) noted a considerable difference between the photometric amplitude in the 1985–1986 data (~0.05 mag) and that found in earlier studies (0.14 mag; Stebbins 1928; 0.15 mag; Belyakina, Burnashev, & Zhilin 1977). If real, these long-term amplitude changes are consistent with the presence of spots undergoing changes in size.

Deviations from a straight bisector are equal to or greater than that of σ Gem but the curvature, as seen in Figure 13, is noticeably different, sometimes curving back and forth. One bisector, obtained at Ritter, exhibits curvature extending far into the wings as was observed in IM Peg. Since the presence of spots on ζ And has not been clearly proved, these results are somewhat surprising. However, the large curvature seen in one CCF extending far into the wings would suggest a rather large spot group. Concurrent photometry is not available but APT

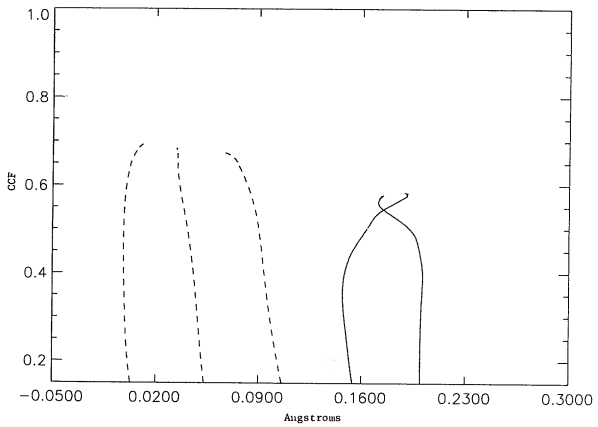

FIG. 13.—Bisectors for ζ And. Again the observations from Kitt Peak are represented by a dashed line and have not been scaled. If P_{orb} is used the phases from left to right would be 0.23, 0.28, 0.34, 0.0, and 0.63 while P_{ph} (Strassmeier et al. 1989) give 0.44, 0.56, 0.67, 0.0, and 0.26. T_0 for both cases is taken to be the date of the first Ritter observation. The template stars were α Ari and α Boo for the Ritter and KPNO data, respectively. The data cover the interval HJD 2,447,899–2,448,029. Axes and arrangement follow the convention of Fig. 11.

data preceding and following the spectroscopic observations reveal variations in amplitude and mean light level.

4.3.5. *UV Coronae Borealis (HD 136901)*

Along with V492 Per and BM CVn, UV CrB was noted to possess significant Ca II emission by Bidelman (1983). Since these were late-type stars with strong Ca II emission, Boyd, Genet, & Hall (1984) obtained photometric observations to determine if spots were present. The light curve of UV CrB displayed quasi-sinusoidal light variations with an amplitude of 0.16 mag. With a spectral type, orbital period (P_{orbit} = 18.6; Fekel et al. 1986) and ΔV similar to that of σ Gem it might be expected that these systems should be much alike. Strassmeier et al. (1989) concluded that ellipticity and reflection dominate the light curve with no apparent effects due to spots. However, Fekel et al. (1989) failed to detect a secondary spectrum, and Hall (1990) demonstrated that the unequal minima actually result from limb-darkening and gravity-darkening effects and not from reflection. Calculations by Hall (1990) based on the ellipsoidal light variations indicate that UV CrB very nearly fills its Roche lobe ($R_* \geq 0.95 R_{Roche}$). Hall (1990) also noted some deviations from his light curve fits and subsequent photometry clearly suggests the presence of spots. Bisectors, showing considerable variation, are plotted in Figure 14. No phase correlation can be determined since less than half of a rotation period was observed including two observations that were obtained 2 months prior to the rest.

An important result from the above discussion of σ Gem, IM Peg, UV CrB, GX Lib, and ζ And is that *the profile variations observed with the cross-correlation technique would be undetectable by other methods* (e.g., changes in line equivalent widths or when the light curve is dominated by ellipticity and reflection effects).

4.4. *Systems with No Profile Asymmetries*

A lack of significant asymmetries in the cross correlations may have resulted from either or both of two effects. For stars with $v \sin i$ less than about 15 km s^{-1} the spectral resolution is inadequate to detect spots even if they cover a large portion of the stellar surface. For a successful detection of a *spot* signature, rotation must dominate the broadening of the line profile which is not the case for $v \sin i < 10$ km s^{-1}. When $v \sin i <$ 10 km s^{-1} other broadening mechanisms become significant and any asymmetries are likely the result of magnetic fields or turbulence. As discussed in § 1, a resolving power greater than 90,000, well above that used here, would be needed to detect such anomalies. Therefore, it is consistent and not surprising that none of the systems with $v \sin i$ less than approximately 15 km s^{-1} displayed asymmetric CCFs. Second, the level of activity at the time of observations is important. Even if the width of the profile is sufficiently large, spots may be too small, too evenly distributed, or have too small a temperature difference compared to the photosphere to produce any significant profile distortions. This appears to be the case for V492 Per, ι Tri, and ε UMi.

5. SPOT MODEL FOR σ GEMINORUM

Not only is it possible to detect the presence of subtle profile asymmetries in spectra of moderate resolution using cross correlation, but the resultant CCF can be inverted or modeled to derive a temperature map of the stellar photosphere. Combining the information contained in the line profile with that contained in broad-band photometry allows the reliable determination of spot latitude, something not possible with photometry alone. The detection of polar spots on V711 Tau and HD 199178 indicates that CA produces results comparable to DI but with lower spatial resolution. To illustrate the capabilities of the CA technique, spot models have been computed for σ Gem.

The modeling programs used here are those of Strassmeier (1986). While more sophisticated algorithms (e.g., maximum entropy) exist, Strassmeier's were quite easy to adapt to correlative analysis. Descriptions of the technique are given in Strassmeier (1988, 1990) with a comparison to maximum entropy methods presented in Strassmeier et al. (1991). Use of two programs (DOPPEL and PROFIL) allow the fitting of the light curve simultaneously with the line profiles. It has been

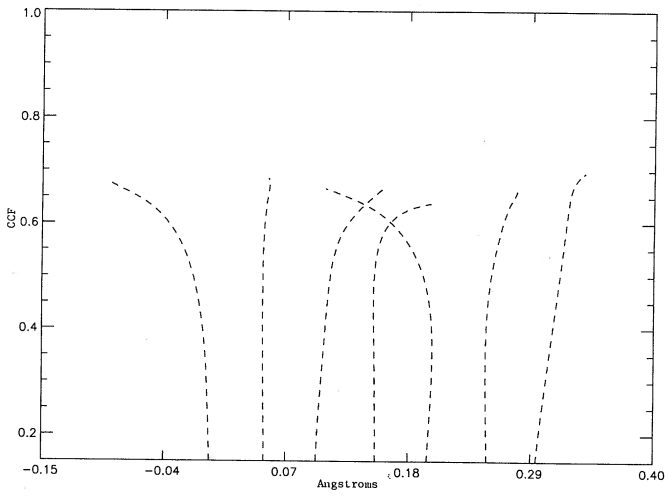

FIG. 14.—Bisectors for UV CrB ordered in phase. Starting phase is taken to be the time of the first observation (HJD 2,447,955). From left to right the phases are 0, 0.15, 0.84, 0.89, 0.94, 1.0, and 0.05. Observations from phases 0 and 0.15 predate the others by 2 months. Bisectors at phases 0.89 and 0.94 are the averages of two and three bisectors, respectively. All observations are from KPNO and cover the interval HJD 2,447, 955–2,448,031. Axes and arrangement follow the convention of Fig. 11.

emphasized by several groups (Noah, Bopp, & Fekel 1987; Jankov & Foing 1987; Strassmeier 1988; Budding & Zeilik 1990) that for reliable mapping photometry must be combined with spectroscopic data. To date, however, Noah et al. (1987) and Strassmeier (1990) were the only investigators to have done so.

The fitting is by trial and error and only a two-temperature model (one for spot and photosphere, respectively) is used. While spot configurations may be rather complicated the results of Strassmeier et al. (1991) and Kürster & Schmitt (1991) support our use of such a simple approach. Every point on the surface of the star is assigned a temperature relative to the quiet photosphere allowing for spots of arbitrary shape. In practice, rectangular spots were adequate for the resolution of our data. Theoretical light curves and rotation profiles are then calculated. Since individual profiles are not directly fitted here, the theoretical rotation profile, calculated by performing a direct disk integration, is convolved with a standard star spectrum to simulate σ Gem. This in turn was cross-correlated with the same template and the resultant CCF compared to the observed CCF at that phase. Microturbulence, macroturbulence, and the instrumental profile are assumed to be identical for the standard, template, and program stars. Changes in the spot distribution are made until a satisfactory fit to both the light curve and the CCFs is obtained. Ideally, a less subjective method of discrimination (e.g., maximum entropy) is preferred and will be considered for future work. However, as seen in Strassmeier et al. (1991), our approach yields essentially the same results as other, more sophisticated algorithms.

Strassmeier (1988) included gravity darkening, reflection, and eclipse effects in his models. However, the secondary of σ Gem has not been detected and there are no indications of eclipses (Strassmeier et al. 1988b). Gravity darkening is thought not to be significant on late-type convective stars (Eaton, Wu, & Rucinski 1980) unless there are considerable deviations from a spherical surface. The separation and rotation rate of the primary are such that this is not likely. Therefore, these effects were ignored.

The modus operandi for fitting is described in detail in Strassmeier (1990). Input physical parameters for σ Gem are those used by Strassmeier et al. (1988b) and subsequently by Olah et al. (1989). Orbital parameters are those of Bopp & Dempsey (1989). The temperature of photosphere and spot were estimated to be 4400 K and $\leq$3870 K, respectively, by Poe & Eaton (1985) using $(V - I)$ observations. Strassmeier et al. (1988a) lowered T_{spot} to 3820 K by using a slightly brighter value for V_0, the unspotted magnitude. Only V-band data were available here so a spot temperature of 3820 K was initially adopted. Since the inclination, i, is not known the value of 60°, used in previous studies, was adopted. The limb darkening coefficient was taken to be 0.73.

Examining the photometry contemporaneous to the CCF observations quickly revealed short term ($\sim$month) changes in the spot distribution. Locations of the photometric minima seem approximately constant but their depths vary considerably. The photometry over the interval HJD 2,447,909–2,447,971 yielded a stable light curve (Fig. 15) that overlapped the majority of the spectroscopic observations and was therefore retained for the final modeling. The spot producing the minimum at $\phi = 0.3$ will be designated as spot A, with B referring to the spot producing the minimum around $\phi = 0.8$.

While fitting the light curve, it soon became clear that with an assigned $T_{spot} = 3820$ K, spot B was much too large to produce the effects seen in the CCFs. Satisfying both types of data required $T_{spot} = 3400$ K. While this spot temperature is about 500 K lower than that found by Poe & Eaton (1985), it lies within the ranges found by other investigators for other stars (Eaton 1991). Furthermore, the temperature of sunspots is known to vary by approximately 300 K over the solar cycle (Maltby et al. 1983). Strassmeier et al. (1988b) noted that their σ Gem photometry at several epochs could be fitted better with spots of temperature 3420 K. For simplicity, both spots were assumed to have the same temperature, although acceptable fits could be obtained with $T_{spot} = 3820$ K for spot A.

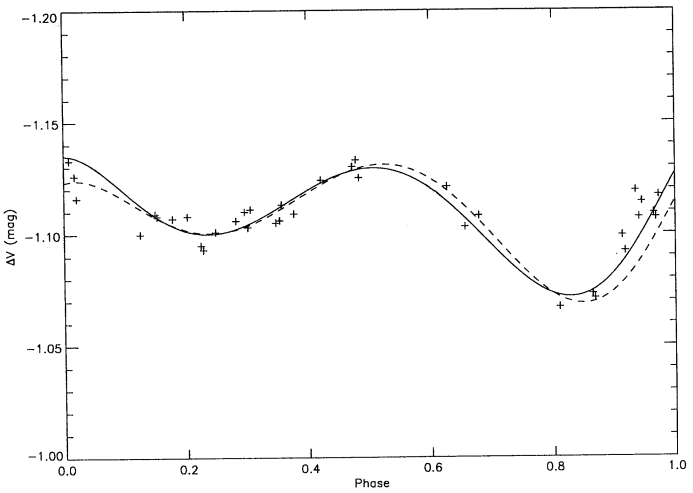

FIG. 15.—Observed photometry of σ Gem (*pluses*) with final theoretical fits (*lines*). The solid line, corresponding to the map in Fig. 16*a*, is the resulting model which most nearly resembles the CCF map. The dashed line represents the overall best fit to the data with the corresponding map displayed in Fig. 16*b*.

The light curve of σ Gem with the computed theoretical fits is shown in Figure 15. Theoretical and observed bisectors are displayed in Figure 10. The resulting maps are displayed in Figures 16 and 17. The solid line in Figure 15 represents the best model which is closest to the corresponding CCF map while the dashed line yields the overall best fit to the photometry. Considering the quality of the photometry the differences are minor as seen in Figure 16 and within errors discussed below. The model in Figure 16*b* will be adopted in subsequent discussions. To compute the theoretical CCFs, spectra of β Oph were used as the standard spectrum to simulate σ Gem. β Oph was broadened by the profiles obtained with PROFIL and cross-correlated with β Gem which was used as the template in the actual correlations. Bisectors which were obtained from Ritter data are quite reasonably reproduced by the model.

Data from KPNO were of lower resolution and therefore cannot be fitted as accurately. Further difficulty arose since no spectra of β Oph were obtained with that instrumentation. To use another standard to model σ Gem would only complicate things unnecessarily. Therefore, Ritter spectra of β Oph were used for the theoretical profiles but with the data resampled, with cubic spline interpolation, to the lower KPNO resolution. Under these circumstances it is not surprising that the fits are not as good. Nonetheless, considerable spatial information can still be extracted.

Both maps indicate the presence of two large, irregularly shaped spots. The spots cover 2.9%–5.4% of the total surface

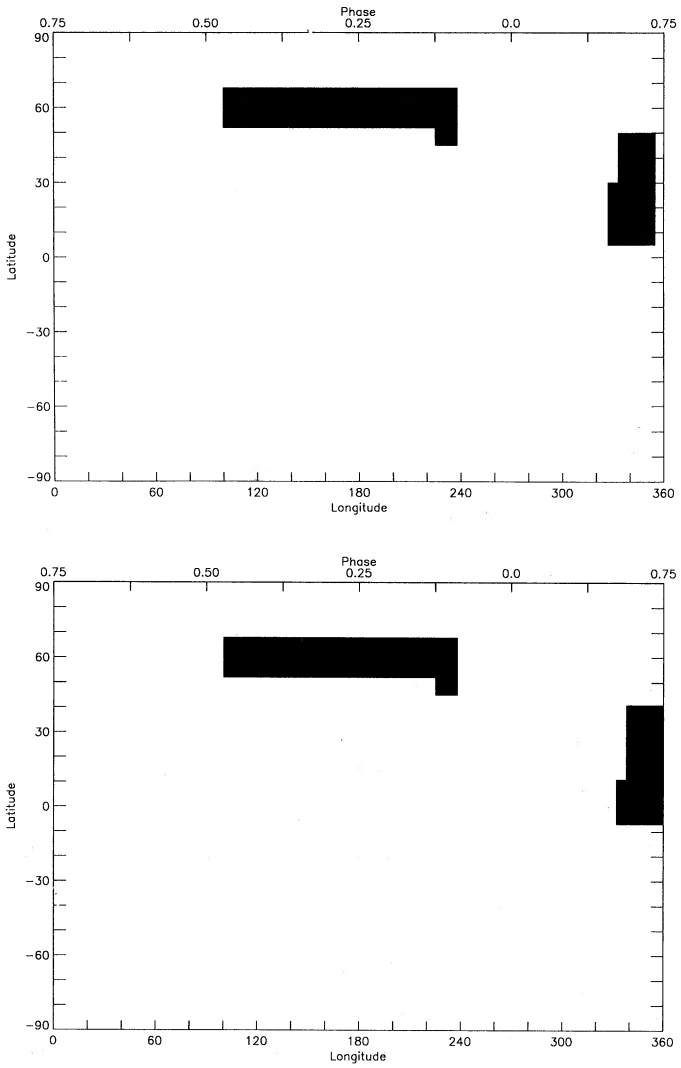

FIG. 16.—Spot maps used to calculate the theoretical fits in Fig. 15. The top map corresponds to the solid line in Fig. 15 while the bottom map produces the dashed fit in the same figure. All spot temperatures were taken to be 3400 K. The irregular shapes were required to fit the asymmetric minima.

in the CCF and photometric models, respectively. Since the positions derived from the CCFs are more reliable, it is clear that both spots lie at high latitude. That the spots on σ Gem lie at high latitude, compared to those on the Sun, is not without precedent. Polar spots were detected with DI on V711 Tau (Vogt 1988), HD 199178 (Vogt 1988), UX Ari (Vogt & Hatzes 1991), and HD 26337 (Strassmeier 1990). Numerous photometric solutions have also indicated the presence of high-latitude spots for several systems (Eaton 1990). Clearly, the dynamo mechanism in these systems is functioning differently than is the case for the Sun.

An additional test was performed to check the reality of the maps. Bisectors were computed assuming no spots were present. The results are shown in Figure 18. At first one would expect the null bisectors to be perfectly straight and indeed those for the Ritter data are nearly so. Both data sets show a leftward bend but with enhanced curvature for the KPNO data. This results because the absorption line depths in the spectra of the standard and program stars are not identical. In the case of HD 199178 this resulted in a sloped CCF. In the

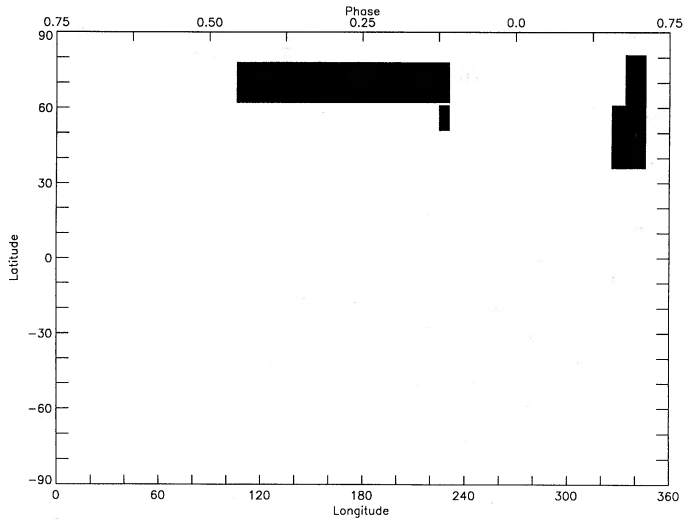

FIG. 17.—Spot map derived from fitting the bisectors in Fig. 10. A small gap appears between the extension and the main body of spot A in the CCF map. This gap is below the resolution threshold and is not significant although it improves the fit.

case of σ Gem the same effect produces a curvature to the bisector. Due to the higher resolution this effect is less noticeable in the Ritter data. Also, since they contain about half the points, the bottom of the KPNO bisectors are heavily weighted by the last point which lies very near the continuum where the error is larger. The variation in the abcissa of the bisector is comparable to that of the Ritter data allowing for the lower resolution. Clearly, the observed and theoretical bisectors which include the spots are distinctly different from those which are "spotless."

Further evidence for the reality of the fits can be seen in Figure 19. Spectral lines of β Oph have been broadened and compared to σ Gem at $\phi = 0.81$ (middle spectrum in Fig. 19). Spectra of σ Gem at this phase correspond to the main photometric minimum and a pseudo-emission bump is visible in the line core. At the top of the figure is a spectrum of β Oph broadened by a rotation profile with no spots present. Below σ Gem is the same spectrum of β Oph broadened by the theo-

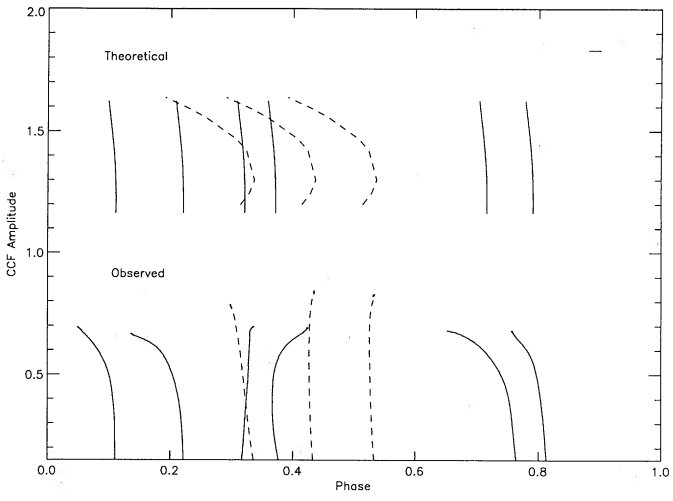

FIG. 18.—Bisectors calculated without the presence of spots. Arrangement is as in Fig. 10. The curvature to the left is the result of spectral type mismatch.

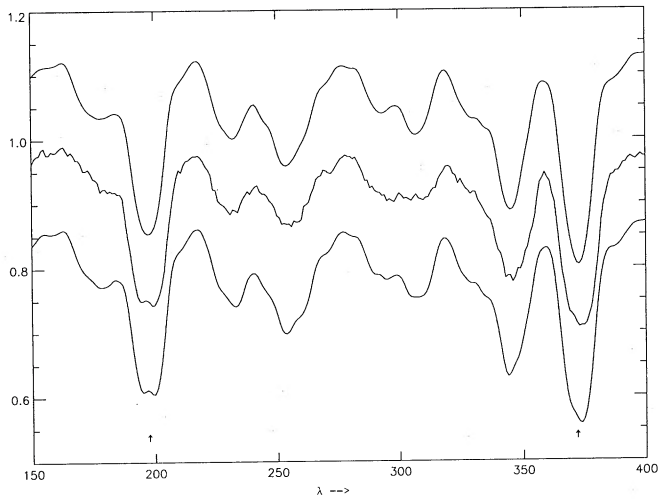

FIG. 19.—Spectra of β Oph and σ Gem in the 6420 Å range. The middle spectrum is that of σ Gem from $\phi = 0.81$. Above this is a spectrum of β Oph broadened with a rotation profile computed with PROFIL but without any spots. A rotation profile computed with the model in Fig. 17 was used to broaden the lower spectrum of β Oph. Arrows mark two "bumps" which clearly result from the spots since they are not observed in the top spectrum. A value of 25 km s^{-1} for $v \sin i$ was used for the rotation.

retical profile calculated with the final spot model. The bumps at the line core are not present in the "spotless' spectrum but are clearly present in the modeled spectrum. Therefore, these "bumps" cannot be the result of noise or other effects but must result from a large spot seen near disk center.

Differences between the photometric and spectroscopic solutions are similar to those detailed by Strassmeier (1990) for HD 26337. Since reliable latitude information is absent in the photometry, the lower positions relative to the CCF map does not present a serious dilemma. The other differences result from uncertainties in V_0, T_{spot}, and i. In fact, the larger spot A could be used for the bisector model with satisfactory results but the smaller size yields a preferable fit. Spot B from the bisector map, however, is necessarily restricted in size by the spectroscopic observations at $\phi = 0.81$.

6. ERRORS AND LIMITS OF CORRELATIVE ANALYSIS

Due to the complexity of the modeling, it is not straightforward to compute formal errors. Some investigators have attempted to estimate errors in the spot models with least squares fitting (e.g., Budding & Zeilik 1987). Strassmeier (1988) performed a parameter study to evaluate the uncertainties in the derived model and he estimated the internal errors in latitude and longitude to be 5° and 2°, respectively, with the spot areas accurate to within 0.5%. Following the same technique of Strassmeier (1988) we derive error estimates which are listed in Table 5. Some values are constrained more than others due to better phase coverage of the CCF observations. Errors for the latitude derive from the bisector fitting only since this parameter is poorly constrained in the photometric solution. The difference in area between the two solutions is about 1.5%, which can be used as an estimate of the uncertainty in spot area.

TABLE 5

SPOT MODEL UNCERTAINTIES FOR σ GEMINORUM

Spot	T_{spot} (K)	Latitude (degrees)	Longitude (degrees)
A.....	±75	±5	±10
B.....	±100	+10 −3	±4

7. COMPARISON WITH PAST RESULTS

The models derived here yield a total spot area of ~5% of the stellar surface of σ Gem. Poe & Eaton (1985) obtained a coverage of 6% in 1980 while Strassmeier et al. (1988b) found a mean spot area of 7% over 9 yr of observations with a range of 3%–12%. Since the latter group fixed T_{spot} at the value of 3820 K, which will require larger spots in general than with the temperature we adopt, it is possible that they may have overestimated some of the spot sizes.

Strassmeier et al. also proposed a 2.7 yr cycle in the spot area observed on σ Gem. Based on their model, a spot area of a little over 5% would be expected for the epoch studied here, in good agreement with our observed value.

8. CONCLUSIONS

The results of this research can be summarized as follows.

1. Cross correlation reliably detects subtle profile asymmetries produced by temperature inhomogeneities in stellar photospheres.

2. CA is well suited for the study of stars with $20 \leq v \sin i \leq 40$ km s^{-1} and periods greater than 10 days.

3. CA can detect the presence of spots when other methods (e.g., photometry and equivalent width variations) fail.

4. The presence of profile asymmetries has been detected for the first time on five long-period RS CVns.

5. Detailed spot maps can be derived from the cross-correlation functions.

6. For the first time spot latitudes on σ Gem have been reliably determined, indicating that the spots lie near the poles.

7. T_{spot} may vary on σ Gem.

It should be kept in mind that correlative analysis is not just some "poor man's" Doppler imaging but rather a totally different technique. Such a method is more practical for the study of long-period systems like σ Gem and IM Peg. For a more complete understanding of the characteristics of spots additional systems in this $v \sin i$ range need to be studied in detail and over long enough intervals to allow the detection of solar-like cycles. Having a possible cycle period of under 3 yr, σ Gem is an ideal candidate for further cross-correlation studies.

We wish to thank Frank Fekel and the referee, Steven Vogt, for their helpful comments on the manuscript. Research at the University of Toledo has been partially supported by NASA grant NAG 5-954. K. G. S. is grateful for the hospitality during his stay at Ritter Observatory and acknowledges partial support through FWF grant P-7993. Research at Tennessee State University was supported by NASA grant NAG 8-111. We are grateful to Myron Smith and Paul Avellar for operating the NSO synoptic program.

REFERENCES

Belyakina, T. S., Burnashev, V. I., & Zhilin, V. M. 1977, Izv. Krymsk. Astrofiz. Obs., 56, 16
Bendat, J. S., & Piersol, A. G. 1986, in Random Data: Analysis and Measurement Procedures (2d ed.; New York: Wiley)
Bernacca, P. L., & Perinotto, M. 1973, Contrib. Oss. Astrof. Univ. Padova in Assiago, 239, 250
Bidelman, W. P. 1983, AJ, 88, 1182
Bopp, B. W. 1982, in Cool Stars, Stellar Systems, and The Sun, ed. M. Giampapa & L. Golub (Washington: Smithsonian Astronomical Observatory), 207
Bopp, B. W., Africano, J. L., Stencel, R. E., Noah, P. V., & Klimke, A. 1983, ApJ, 275, 691
Bopp, B. W., & Dempsey, R. C. 1989, PASP, 101, 516
Bopp, B. W., Dempsey, R. C., & Maniak, S. 1988, ApJS, 68, 803
Bopp, B. W., Dempsey, R. C., Morrison, N. D., Burmeister, R. J., & Jones, R. A. 1989, BAAS, 21, 759
Bopp, B. W., & Talcott, J. C. 1980, AJ, 85, 55
Boyd, L. J., Genet, R. M., & Hall, D. S. 1984, Inf. Bull. Var. Stars, 2546
Budding, E., & Zeilik, M. 1987, ApJ, 319, 827
———. 1990, in Active Close Binaries, ed. C. Ibanoglu (Dordrecht: Kluwer), 831
Burke, E. W., Baker, J. E., Fekel, F. C., Hall, D. S., & Henry, G. W. 1982, Inf. Bull. Var. Stars, 2111
Collier-Cameron, A. C. 1991, in Surface Inhomogeneities in Late-Type Stars, ed. P. Byrne & D. Mullan (Berlin: Springer), in press
Dempsey, R. C. 1991, Ph.D. thesis, University of Toledo
Deutsch, A. 1970, ApJ, 159, 985
Donati, J.-F., Brown, S. F., Semel, M., Dempsey, R. C., Rees, D. E., Mathews, J. M., Hall, D. S., Henry, G. W., & Bopp, B. W. 1992, A&A, submitted
Eaton, J. 1990, Info. Bull. Var. Stars, 3460
———. 1991, in Surface Inhomogeneities in Late-Stars, ed. P. B. Byrne & D. J. Mullan (Berlin: Springer) in press
Eaton, J. A., Wu, C. C., & Rucinski, S. M. 1980, ApJ, 239, 919
Eker, Z. 1986, MNRAS, 221, 947
Engvold, O., Ayres, T. R., Elgaroy, O., Jensen, E., Jordas, P. B., Kjeldseth-Moe, O., Linsky, J. L., Schnopper, H. W., & Westergaard, H. J. 1988, A&A, 192, 234
Fekel, F. C. 1991, private communication
Fekel, F. C., Kirkpatrick, J. D., Yang, X., & Strassmeier, K. G. 1989, AJ, 97, 202
Fekel, F. C., Moffett, T. J., & Henry, G. W. 1986, ApJS, 60, 551
Fried, R. E., et al. 1983, Ap&SS, 93, 305
Genet, R., M., Boyd, L. J., Kissell, K. E., Crawford, D. L., Hall, D. S., Hayes, D. S., & Baliunas, S. L. 1987, PASP, 99, 660
Gray, D. F. 1989, ApJ, 347, 1021
Hall, D. S. 1976, in Multiple Periodic Variable Stars, ed. W. S. Fitch (Dordrecht: Reidel), 287
———. 1981, in Solar Phenomena in Stars and Stellar Systems, ed. R. M. Bonnet & A. K. Dupree (Dordrecht: Reidel), 431
———. 1990 AJ, 100, 554
Hatzes, A. P., Penrod, D., & Vogt, S. 1989, ApJ, 341, 456
Hoffleit, D. 1982, The Bright Star Catalog (New Haven: Yale Observatory)
Jankov, S., & Foing, B. 1987, in Cool Stars, Stellar Systems, and The Sun, ed. J. Linsky & R. Stencel (New York: Springer), 528
Jetsu, L., Huovelin, J., Tuominen, I., Vilhu, O., Bopp, B. W., & Piirola, V. 1990, A&A, 236, 423
Kürster, M., & Schmitt, J. H. M. M. 1991, in IAU Colloq. 130, The Sun and Cool Stars: Activity, Magnetism, Dynamos, ed. I. Tuominen, D. Moss, & G. Rudiger (Berlin: Springer), in press
Maltby, P., Albregtsen, F., Kjeldseth, O., Kurucz, R., & Avrett, E. 1983, in Cool Stars, Stellar Systems, and the Sun, ed. S. Baliunas & L. Hartmann (New York: Springer), 259
Moore, C. E., Minnaert, M. G., & Houtgast, J. 1966, The Solar Spectrum 2935 Å to 8770 Å (NBS Monograph 61)
Neff, J. 1990, in Active Close Binaries, ed. C. Ibanoglu (Dordrecht: Kluwer), 809
Noah, P., Bopp, B. W., & Fekel, F. 1987, in Cool Stars, Stellar Systems, and The Sun, ed. J. Linsky & R. Stencel (New York: Springer), 505
Noyes, R. W., Hartmann, L. W., Baliunas, S. L., Duncan, D. K., & Vaughn, A. N. 1984, ApJ, 279, 763
Olah, K., Panov, K. P., Pettersen, B. R., Valtaoja, E., & Valtaoja, L. 1989, A&A, 218, 192
Piskunov, N. E., Tuominen, I., & Vilhu, O. 1990, A&A, 230, 363
Poe, C., & Eaton, J. 1985, ApJ, 289, 644
Rodono, M., et al. 1987, A&A, 176, 267
Smith, S. E., & Bopp, B. W. 1982, Astrophys. Lett., 22, 127
Soderblom, D., Pendleton, J., & Pallavicini, R. 1989, AJ, 97, 539
Stebbins, J. 1928, Pub. Washburn Obs., 15, 29
Strassmeier, K. G. 1986, Ph.D., Universität Graz
———. 1988, A&SS, 140, 223
Strassmeier, K. G., et al. 1988b, A&A, 192, 135
———. 1990, ApJ, 348, 682
Strassmeier, K., Hall, D., Boyd, L., & Genet, R. 1989, ApJS, 69, 141
Strassmeier, K. G., Hall, D. S., Zeilik, M., Nelson, E., Eker, Z., & Fekel, F. C. 1988a, A&AS, 72, 291
Strassmeier, K. G., Rice, J. B., Wehlau, W. H., Vogt, S. S., Hatzes, A. P., Tuominen, I., Piskunov, N. E., Hackman, T., & Poutanen, M. 1991, A&A, in press
Strassmeier, K. G., Weichinger, S., & Hanslmeier, A. 1986, Info. Bull. Var. Stars, 2937
Strassmeier, K. G., et al. 1988b, A&A, 192, 135
Toner, C., & Gray, D. F. 1988, ApJ, 334, 1008
Vogt, S. S. 1988, in The Impact of Very High S/N Spectroscopy on Stellar Physics, ed. G. Cayrel de Stroebel & M. Spite (Dordrecht: Kluwer) 253
Vogt, S. S., & Hatzes, A. P. 1991, in IAU Colloq. 130, The Sun and Cool Stars: Activity, Magnetism, Dynamos, ed. I. Tuominen, D. Moss, & G. Rudiger (Berlin: Springer), 297
Vogt, S. S., & Penrod, D. 1983, PASP, 95, 565
Vogt, S. S., Penrod, D., & Hatzes, A. 1987, ApJ, 321, 496